

## Helically coiled cage forms of graphitic carbon

Sigeo Ihara and Satoshi Itoh

*Central Research Laboratory, Hitachi Ltd., Kokubunji, Tokyo 185, Japan*

Jun-ichi Kitakami

*Hitachi VLSI Engineering Corp., Kodaira, Tokyo 187, Japan*

(Received 14 May 1993)

Helically coiled forms of the carbon cage on the nanometer scale are theoretically proposed. The optimized surface construction for different types of helically coiled structures consisting of sevenfold, sixfold, and fivefold rings of carbon atoms is given. The thermal stability of various helical structures is studied by molecular-dynamics simulations, employing Stillinger-Weber-type potentials. The structures are found to be thermodynamically stable. It is found that the helically coiled structures derived from toroidal structures  $C_{360}$  and  $C_{1080}$  are stiff, so that the ring pattern of the surface changes with pitch length. On the contrary, the structure derived from torus  $C_{540}$  is found to be soft, i.e., a change in the pitch length does not change the ring pattern of the surface.

### I. INTRODUCTION

Various graphite carbon forms, which are promising materials in future technology, have been proposed by many researchers. In the positively curved surfaces observed in fullerene  $C_{60}$  (Ref. 1) and carbon nanotubes,<sup>2</sup> fivefold and sixfold rings of carbon atoms are present. Recently, carbon forms with periodic minimal surfaces have been theoretically proposed,<sup>3-5</sup> in which the introduction of sevenfold or eightfold rings into sixfold rings gives rise to a negatively curved surface. Transmission electron microscope studies by Iijima, Ichihashi, and Ando<sup>6</sup> experimentally revealed that sevenfold rings play an important role in the growth of negatively curved surface of tubes. By combining the positively curved and negatively curved surfaces appropriately, we have recently proposed a structure of the toroidal carbon form,  $C_{360}$  (Ref. 7) with  $D_{5d}$  symmetry: Molecular-dynamics simulations showed that the toroidal structure  $C_{360}$ , and other structures derived from  $C_{360}$ , are thermodynamically stable. By connecting carbon tubes, different types of toroidal structures,  $C_{540}$  and  $C_{576}$  with  $C_{6v}$  symmetry, have also been recently proposed by Dunlap.<sup>8</sup>

In this paper, we propose helically coiled forms of the carbon cage on the nanometer scale, which can, in a topological sense, be derived from tubes or tori. Some of the helical forms are expected to manifest themselves in tube forms by coiling around a fiber axis to reduce strain energy. Here, we provide a theoretical prescription for creating nanometer-scale helices using the toroidal structures and study the properties of these structures. The motivation behind this study is as follows: (1) the electrical or elastic properties may be modulated by the writhing or twisting<sup>9</sup> in addition to changing the diameters (of cross section) and the degree of helical arrangement as in tubes;<sup>2</sup> (2) a helical structure is mechanically stable under axial, shearing, torsional, and bending forces (moments), as frequently seen in nature (DNA, spirillum, a kind of prokaryotic cell, beanstalk, etc.) and in man-made

mechanical structures (spring coil, etc.); and (3) a variety of helical structures can be formed: for instance, a helix with a curved axis can form a different helix of higher order, a supercoil or super-supercoil. If the synthesis of these structures is controlled, helical forms of carbon will become useful.

### II. SIMULATION OF HELICALLY COILED CARBON STRUCTURES

#### A. Construction of geometry

In order to construct a helical structure by tiling the optimized pattern of the carbon rings, the following method was used. Along the radius of curvature, the torus consisting of the optimized pattern of carbon rings is cut into small pieces, which are stretched toward the fiber axis, and combined continuously to obtain the initial atomic positions of the helical structures. The helix is created so that one pitch contains one torus. In order to compare the properties of helical structures with different forms, three types of toroidal structures were prepared: torus  $C_{540}$  proposed by Dunlap and tori  $C_{360}$  and  $C_{1080}$  proposed by us. By applying Goldberg's algorithm,<sup>10</sup> sixfold rings are inserted into the original structure, and the directions of the fivefold and sevenfold rings are turned appropriately as the size increases, so torus  $C_{1080}$  is derived from torus  $C_{360}$ . Hereafter, we use helix  $C_n$  to denote a helix consisting of one torus ( $C_n$ ) in one pitch, where  $n = 360, 540,$  and  $1080$ .<sup>11</sup>

#### B. Description of molecular-dynamics simulations

Molecular-dynamics simulations were employed to obtain the optimized ground-state structure as well as the tensioned structure. The Stillinger-Weber type three-body potentials,<sup>12</sup> which are also useful in carbon atoms, were used. The following parameters, which are optimized for graphite,<sup>13</sup> were used:  $A = 5.373\ 203\ 7$ ,  $B = 0.508\ 245\ 1$ ,  $a = 1.894\ 361\ 9$ ,  $\lambda = 18.707\ 929$ , and

$\gamma=1.2$ . In the three-body term, the constant  $\frac{1}{3}$  is replaced by  $\frac{1}{2}$  to represent the honeycomblike structure. Periodic boundary conditions were applied in all directions. The open helical structures were placed in the center of a large computational box, whose side is at least 3 times longer than the structure. The integration of the equations of motion for atomic coordinates was performed by a leap-frog algorithm with a time step of 0.36 fs. Simulation runs, comprising 2000 time steps (0.72 ps), were used for the relaxation of the atoms, in which the velocities at every step were rescaled for the first 1000 steps. Thereafter, atoms were relaxed more gradually. For the calculation of the cohesive energy of the ground state, the system was cooled down to 0 K in several thousand steps by using the first-order equations of motion (dynamical steepest descent method). Less than  $10^{-12}$  J/m of force acting on an atom was used as the convergence criterion. This criterion was also used in the *tension test* (comprising up to a few hundred thousand steps for each coil length) where the spring constants were evaluated by calculating the coil lengths and the total energies of the helices under tension along the fiber axis using a quenching procedure. Here one edge of the helical structure was fixed during the simulation of tensioning (stretching or compressing) of coiled structures. The usual second-order equations of motion were employed for the high-temperature simulations comprising 20 000 steps, the temperature was gradually raised to 2000 K in 15 000 steps with total energy being observed after 16 000 steps. To eliminate the edge effect, we used the energies of a pitch in the center of the helical struc-

ture.<sup>14</sup> Helices of two pitches and five pitches (which correspond to 720 and 1800 atoms for helix  $C_{360}$ ) provided the same results as for one central pitch within the computational error. Although the potentials are empirical, we believe that the qualitative predictions mentioned below are reasonable.

### III. RESULTS AND DISCUSSIONS

#### A. Optimized tilting of carbon rings of helix $C_{360}$

First, the change of the ring pattern from the toroidal structure to helically coiled one is studied. Using helix  $C_{360}$ , the stability ring patterns along the inner ridge line for the helical structure with a low pitch angle are studied in detail. With different initial velocities for the same initial positions for the helix  $C_{360}$  prepared as mentioned before, at least three types of ring patterns are observed in our simulations [see Figs. 1(a) and 2]: Type *A*, two fivefold rings and two eightfold rings periodically appear in the sixfold rings [Fig. 2(a)]; type *B*, buckled sixfold rings and fivefold rings with tetrahedral bonds appear [Fig. 2(b)]; and type *C*, two sevenfold rings appear in the sixfold rings [Fig. 2(c)]. Note that in type *C*, depicted in Fig. 2, sixfold rings occupy preferentially around fivefold and sevenfold rings as in the inner circle of the toroidal structure  $C_{360}$  depicted in Fig. 3(a) though the patterns are different in torus and helix. [The numbers of fivefold, sixfold, and sevenfold rings per 360 atoms in the type *C* helical structure are the same as in the torus  $C_{360}$  (Ref. 7).] The diameters of the inside and outside circles of

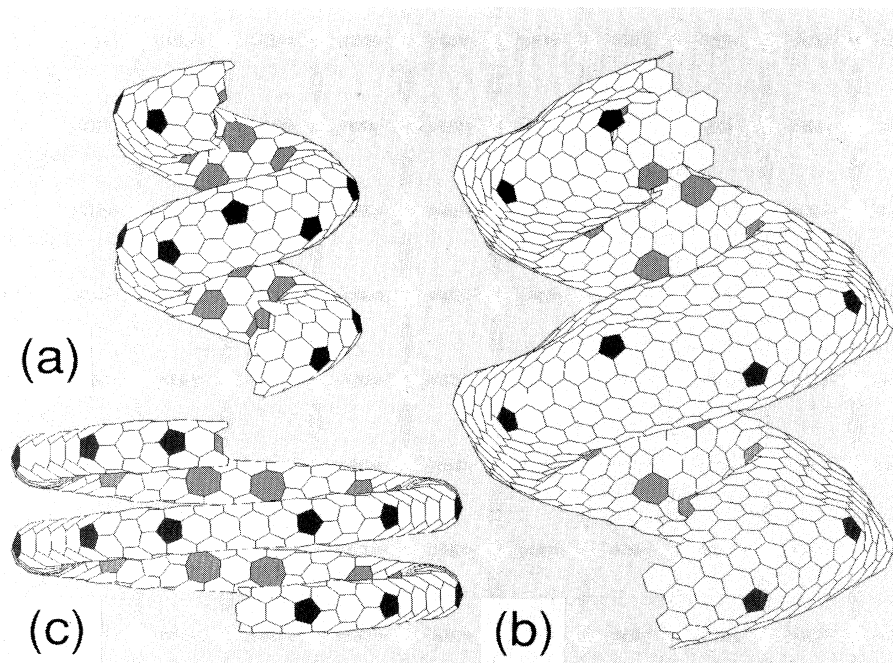


FIG. 1. The helical cage forms of carbon that have the lowest cohesive energy per atom (only two pitch lengths are shown). (a) Helix  $C_{360}$ , (b) helix  $C_{1080}$ , and (c) helix  $C_{540}$ . The fivefold and sevenfold rings (shaded) appear in the outer and inner ridge lines, respectively, amid a background of the sixfold rings. Here rings are constructed by connecting the nearest-neighbor sites of the carbon atoms.

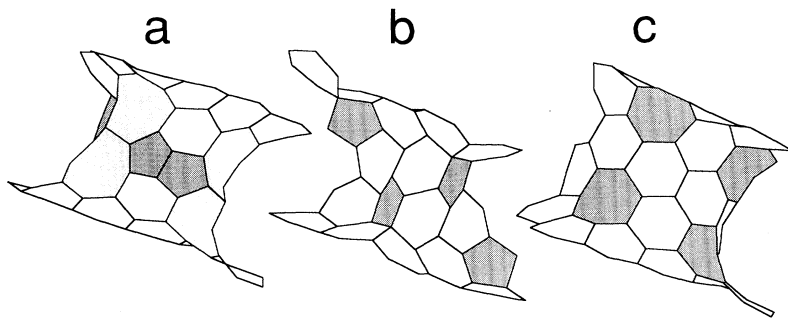


FIG. 2. The patterns that appear in the inner ridge line of the helical cage form of carbon. Structures containing pattern (a) consisting of fivefold and eightfold rings are metastable, structures containing pattern (b) consisting of fivefold and sixfold rings are also metastable, while structures (such as those shown in Fig. 1) containing pattern (c) consisting of sixfold and sevenfold rings are stable.

these helices (projected onto the vertical plane of the fiber axis) are 7.8 Å and 22.6 Å, respectively, which are close to those in the torus  $C_{360}$ . The cohesive energies per atom of the three types of helices, *A*, *B*, and *C*, calculated by quenching using molecular-dynamics simulations are  $-7.37$ ,  $-7.39$ , and  $-7.41$  eV, respectively. The type *C* structure is energetically the most stable of the three, as mentioned before.

Dynamical simulations for three types of helices of  $C_{360}$ , at 300 K and at higher temperatures (up to 1500 K) were also performed. The type *C* of helix  $C_{360}$  was stable at 300 and 1500 K although it shrinks several percent along the fiber axis, and collapses at temperatures exceeding 1500 K. Types *A* and *B* of helix  $C_{360}$  become unstable and collapse at 300 K. This confirms that the type *C* structure is thermodynamically stable and that the others are local minima. Since the systems of two and five pitches provide results similar to those for a central pitch of type *C* of helix  $C_{360}$ , the results obtained here are applicable to the extended infinite system.

### B. Properties of stable helical structures

The optimized (and lowest energy) structures of three types of helical structures, helices  $C_{360}$ ,  $C_{1080}$ , and  $C_{540}$  (of centered two pitches for low pitch angle), obtained by molecular-dynamics simulations are shown in Fig. 1. The helical structures obtained here are right handed; however, it is possible to form left-handed helices. It should be noted that for helix  $C_{540}$  there seems to be no pattern dependence like helices  $C_{360}$  as we discussed in previous sections. The helically coiled form of  $C_{540}$  seems to be created without pattern change with rebondings. The geometrical parameters, total energies, and the spring constants for helices  $C_{360}$ ,  $C_{1080}$ , and  $C_{540}$  are shown in Table I. The values of lowest cohesive energies per atom of helices  $C_{360}$ ,  $C_{1080}$ , and  $C_{540}$  of the central one pitch

and those of corresponding toroidal structures are almost the same:  $-7.41$ ,  $-7.43$ , and  $-7.39$  eV. This may be due to the fact that the local and global networks of the rings of these structures are similar to each other. Note that the cohesive energy of the fullerene  $C_{60}$  is  $-7.29$  eV/atom and that of the graphite sheet is  $-7.44$  eV/atom. The cohesive energies of the helical carbon forms are lower than that of the stable  $C_{60}$ . This indicates that those helical forms are energetically stable. Since torus  $C_{1080}$  is derived from torus  $C_{360}$ , the lower value of the cohesive energy of helix  $C_{1080}$  than that of helix  $C_{360}$  may be attributed to the larger number of sixfold rings in helix  $C_{1080}$ . Since the system of two and five pitches provide results similar to those for a central pitch of helix, the results obtained here are likely to hold for an infinitely extended system such as carbon whiskers, filaments, or fibers.<sup>15</sup>

Dynamical simulations for these types of helices, type *C* of  $C_{360}$ ,  $C_{540}$ , and  $C_{1080}$ , at 300 K and at higher temperatures (up to 1500 K) were also performed. The helices  $C_{540}$ , type *C* of  $C_{360}$  and  $C_{1080}$ , were stable at 300 and 1500 K although they shrink several percent along the fiber axis, and they collapse at temperatures exceeding 1500 K. This confirms that these helical structure are thermodynamically stable.

The helical structures of lowest energy obtained by optimization used here consist of pairs of fivefold and sevenfold rings and of sixfold rings. Along the outer ridge line of helices  $C_{360}$ ,  $C_{540}$ , and  $C_{1080}$ , fivefold rings appear to create positive curvature in the same fashion as in the corresponding toroidal structures. In the outer ridge line of these helical structures, no rebonding of fivefold and sixfold rings is observed when helical structures are created from the toroidal ones. On the other hand, along the inner ridge line of these helical structures, various patterns appear in representing negatively curved surface: for the helix  $C_{540}$ , the ring pattern of sevenfold and six-

TABLE I. The values of lowest cohesive energies per atom, spring constants, and geometrical parameters of helices  $C_{360}$ ,  $C_{540}$ , and  $C_{1080}$  of central one pitch (see text). The radii of the inside and outside circles of these helices  $R_0$  and  $R_1$  are the projected ones onto the vertical plane of the fiber axis.

Structure	Energy (eV)	Coil length	$R_0$ (Å)	$R_1$ (Å)	$k$ ( $10^{-4}$ eV/Å)	$\cos\alpha$	$G$ (GPa)
helix 360	$-7.41$	12.9	11.5	3.5	8.0	0.409	0.43
helix 540	$-7.39$	8.5	20.7	14.7	6.0	0.16	0.53
helix 1080	$-7.43$	22.1	20.4	6.3	14.1	2.87	0.31

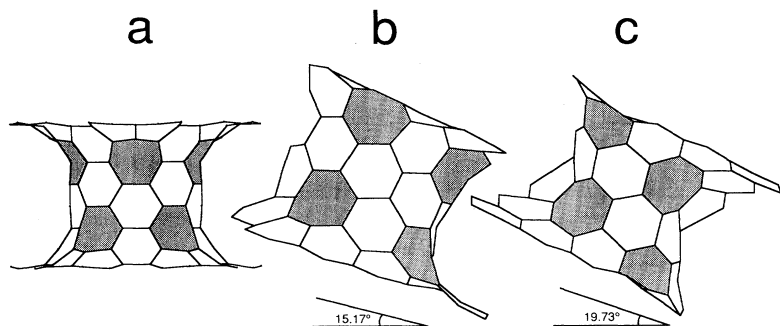


FIG. 3. The pattern transformation of the sevenfold rings with different angles. Here pitch  $\alpha$  increases from (b)  $15.17^\circ$  to (c)  $19.73^\circ$ , without changing the cohesive energy. For clarity, the pattern that appears in the inner circle of the torus  $C_{360}$  is shown in (a).

fold rings is the same as in the toroidal structure,<sup>8</sup> while for the helices  $C_{360}$  and  $C_{1080}$ , rebondings of carbon atoms between rings in the inner ridge line are observed when helical structures are created from the toroidal ones. This pattern transformation of carbon rings indicates that a kind of plastic deformation occurs along the inner ridge line in stabilizing these helices when they are created from the toroidal ones.

### C. Elastic properties and tensioned structures of helices

The elastic properties for helices  $C_{360}$ ,  $C_{540}$ , and  $C_{1080}$  were examined using the results of the *tension test* performed by molecular dynamics. From the relation of the total energy change versus coil length, the spring constants of the helical structures per pitch are obtained numerically. The results are given in Table I. The values of the spring constants for helices  $C_{360}$  and  $C_{1080}$  are larger than that for helix  $C_{540}$ . Helices  $C_{360}$  and  $C_{1080}$  are found to transform to other structures with rebonding of the atoms on the surface with increasing the pitch length or pitch angle. This indicates that they are so stiff that a kind of plastic deformation also occurs along the inner ridge line. Moreover, it is found that while the pattern of the fivefold rings is preserved, the pattern reformations of the sevenfold rings in these helical structures occur discretely with increasing pitch angle  $\alpha$  (from one stable pitch angle to another) as illustrated in Fig. 3. (Note that the pattern of sevenfold rings for the helix  $C_{540}$  could be obtained as an infinitely stretched form of the helix  $C_{360}$ -type structure.) Conversely, there is no minimum for the helix  $C_{540}$  until collapse (the closely coiled form extrapolated at  $\alpha=0$ ). The increase in the coil energy with increasing  $\alpha$  is very small, and the spring constant is also very small as can be seen in Fig. 4. Owing to the small increase in the coil energy, it is possible to have relatively large values of  $\alpha$  which correspond to the open-coiled form of helix  $C_{540}$  without changing the ring pattern of the carbon atoms. Even supercoiled or super-supercoiled forms with the same ring pattern could be constructed. From Table I, we can conclude that the difference in elasticity of the helically coiled forms discussed above is attributed to the difference in patterns of the sevenfold rings which depend on the geometrical properties such as ratio of radii of cross section and curvature.

To gain better qualitative understanding of the above conjecture, the formula of the spring constant of the con-

tinuum theory was applied to evaluate the shearing moduli for these helical structures. For an  $m$ -coiled helix, the spring constant  $k$  is given by<sup>16</sup>

$$k = \frac{\cos\alpha}{\left[ \frac{\cos^2\alpha}{GI_t} + \frac{\sin^2\alpha}{EI_b} \right] 2m\pi R^3},$$

where  $R$  is the radius of curvature defined by  $R = (R_0 + R_1)/2$ , and  $R_0$  and  $R_1$  are the outer and inner radii of curvature, respectively. Here  $\alpha$ ,  $E$ , and  $G$  stand for the pitch angle, Young's modulus, and shear modulus, respectively;  $I_b$  and  $I_t$  stand for the bending and torsional moments of inertia, where  $I_t = 2I_b$ , and  $I_t = \pi(d_0^4 - d_1^4)/32$  for helically coiled cage forms. Here  $d_0$  and  $d_1$  are the outer and inner cross-sectional radii, and  $d_0 - d_1$  provides the thickness of the graphite monolayer, using  $d_0 - d_1 = 1 \text{ \AA}$ . For our cases,  $\cos\alpha$  ranges from 0.96 to 0.99, thus making the second term vanish, so  $G$  can be obtained by estimating the spring constant  $k$  (for  $m=1$ ) from Fig. 4. Although the spring constants for helices  $C_{360}$ ,  $C_{540}$ , and  $C_{1080}$  range over one order of magnitude, the values of shear moduli for these structures, which are one order smaller than for the micrometer-scale carbon fiber,<sup>17</sup> are quite close. Thus we can conclude the main factor in changing the values of  $k$  is the difference in the geometrical pattern of the rings.

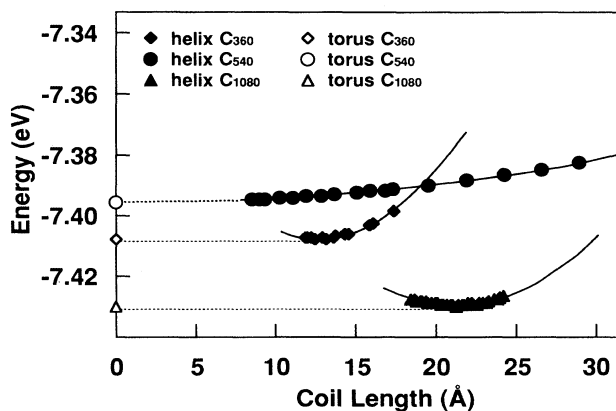


FIG. 4. The energies of the helical structures vs coil length of one pitch.

## IV. CONCLUSIONS

We showed that various forms of helically coiled structures are possible, which are energetically and thermodynamically stable, if they are formed. Though the formation process of these structures is not the subject of this work, the variety of patterns in the inner ridge line of the helical structures indicates that there exist many different coiled forms of stable cage carbon structures and that they may be able to transform into other forms. It would be interesting if the proposed structure and its variant forms—the supercoiled structure, helical coiling of the tube, nested helical forms, and the double and triple helices observed in biological systems—could be constructed from the graphitic carbon cage. The forms of

spiral of Archimedes, and the equiangular and logarithmic ones are also the natural extension of our helically coiled structures since they can be easily obtained by a similar procedure. We have found that the elastic properties of helical forms are modulated by the pitch angle, which changes the degree of writhing and twisting, and also by the diameters of the tube. It is worth mentioning that this mechanical modulation will lead to changes in the electrical properties as in tubes.<sup>2</sup>

## ACKNOWLEDGMENTS

We wish to acknowledge helpful discussions with D. Pines, S. Ichimaru, M. Yamane, S. Nagashima, S. Miyamoto, I. Doi, I. Ihara, and B. M. Patil.

- 
- <sup>1</sup>H. W. Kroto, J. R. Heath, S. C. R. F. Curl, and R. E. Smalley, *Nature* (London) **318**, 162 (1985); W. Krätschmer, L. D. Lamb, K. Fostiropoulos, and D. R. Huffman, *ibid.* **347**, 354 (1990).
- <sup>2</sup>S. Iijima, *Nature* (London) **354**, 56 (1991); R. Saito, M. Fujita, G. Dresselhaus, and M. S. Dresselhaus, *Phys. Rev. B* **45**, 6234 (1992); T. W. Ebbesen and P. M. Ajayan, *Nature* (London) **358**, 220 (1992); J. W. Mintmire, B. I. Dunlap, and C. T. White, *Phys. Rev. Lett.* **68**, 631 (1992); N. Hamada, S. Sawada, and A. Oshiyama, *ibid.* **68**, 1579 (1992); R. Saito, M. Fujita, G. Dresselhaus, and M. S. Dresselhaus, *Appl. Phys. Lett.* **60**, 2204 (1992); D. H. Robertson, D. W. Brenner, and J. W. Mintmire, *Phys. Rev. B* **45**, 12 592 (1992).
- <sup>3</sup>A. L. Mackay and H. Terrones, *Nature* (London) **352**, 762 (1991).
- <sup>4</sup>D. Vanderbilt and J. Tersoff, *Phys. Rev. Lett.* **68**, 511 (1992).
- <sup>5</sup>T. Lenosky, X. Gonze, M. P. Teter, and V. Elser, *Nature* (London) **355**, 333 (1992); S. J. Townsend, T. J. Lenosky, D. A. Muller, C. S. Nichols, and V. Elser, *Phys. Rev. Lett.* **69**, 921 (1992); R. Phillips, D. A. Drabold, T. Lenosky, G. B. Adams, and O. F. Sankey, *Phys. Rev. B* **46**, 1941 (1992).
- <sup>6</sup>S. Iijima, T. Ichihashi, and Y. Ando, *Nature* (London) **356**, 776 (1992); S. Iijima, P. M. Ajayan, and T. Ichihashi, *Phys. Rev. Lett.* **69**, 3100 (1992).
- <sup>7</sup>S. Itoh, S. Ihara, and J. Kitakami, *Phys. Rev. B* **47**, 1703 (1993); S. Ihara, S. Itoh, and J. Kitakami, *ibid.* **47**, 12 908 (1993).
- <sup>8</sup>B. I. Dunlap, *Phys. Rev. B* **46**, 1933 (1992).
- <sup>9</sup>W. R. Bauer, F. H. C. Crick, and J. H. White, *Sci. Am.* **243**, 100 (1980); F. H. C. Crick, *Proc. Natl. Acad. Sci. U.S.A.* **73**, 2639 (1976).
- <sup>10</sup>M. Goldberg, *Tohoku Math. J.* **43**, 104 (1937).
- <sup>11</sup>Although torus C<sub>576</sub> is thermodynamically stable, helix C<sub>576</sub> turned out to be thermodynamically unstable by our dynamical calculations.
- <sup>12</sup>F. H. Stillinger and T. A. Weber, *Phys. Rev. B* **31**, 5262 (1985); **33**, 1451(E) (1986).
- <sup>13</sup>F. F. Abraham and I. P. Batra, *Surf. Sci.* **209**, L125 (1989).
- <sup>14</sup>Since our interest lies in the “bulk” properties of the helix, the effects of the open ends, which may be covered with some form of carbon residue as in the case of tubes, are excluded as much as possible. However, in our high-temperature simulations, atoms at the open ends bend inwards to cover the open end. In helix C<sub>540</sub>, the open end is covered with sevenfold rings.
- <sup>15</sup>G. G. Tibbetts, *J. Cryst. Growth* **66**, 632 (1984); J. S. Speck, M. Endo, and M. S. Dresselhaus, *ibid.* **94**, 834 (1989).
- <sup>16</sup>A. Okumura, *Strength of Materials* (Corona Pub, Tokyo, 1958), p. 325 (*Zairyō Rikigaku*, in Japanese).

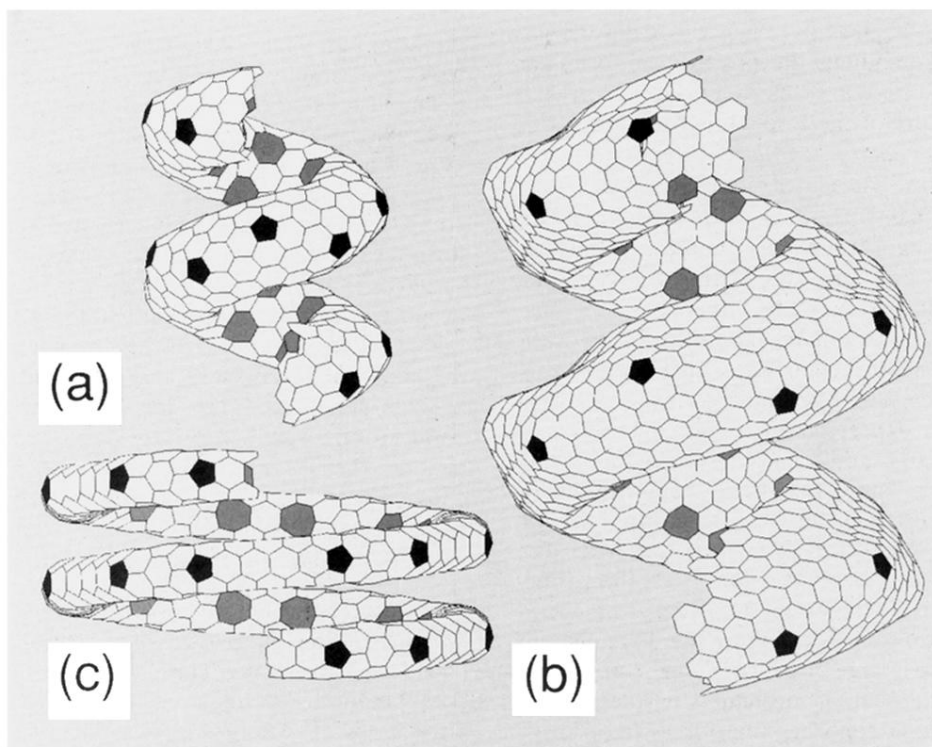


FIG. 1. The helical cage forms of carbon that have the lowest cohesive energy per atom (only two pitch lengths are shown). (a) Helix  $C_{360}$ , (b) helix  $C_{1080}$ , and (c) helix  $C_{540}$ . The fivefold and sevenfold rings (shaded) appear in the outer and inner ridge lines, respectively, amid a background of the sixfold rings. Here rings are constructed by connecting the nearest-neighbor sites of the carbon atoms.